Signal Processing Techniques Used in the ARM 8-mm Cloud Radars

K. P. Moran, R. Lataitis, M. J. Post, B. E. Martner, and D. Welsh
National Oceanic and Atmospheric Administration
Environmental Technology Laboratory
Boulder, Colorado

D. Strauch
Cooperative Institute for Research in the Environmental Sciences
Boulder, Colorado

K. B. Widener
Pacific Northwest National Laboratory
Richland, Washington

Introduction

The Atmospheric Radiation Measurement (ARM) Program's Millimeter Wavelength Cloud Radars (MMCRs) are a new generation of research tools designed to provide high temporal and spacial resolution measurements of the clouds above the Cloud and Radiation Testbed (CART) sites. The last of the four field sites for the MMCRs, located on Manus Island, Papau New Guinea, will be operating in 1999, completing the first phase of installations. Other sites already in operation include the Southern Great Plains (SGP), the North Slope of Alaska (NSA), and the Republic of Nauru. The use of large aperture high-gain antennas, coherent pulse integration, and pulse compression provide a radar with excellent sensitivity (Moran et al. 1998; Clothiaux et al. 1999). These techniques each require special processing to improve the data products and reduce the influence of unwanted side effects. In this paper, we briefly examine the MMCR signal processing techniques that combine to provide accurate estimates of radar reflectivity.

Radar Processing Blocks

The radar's receiver and signal processing software is composed of a collection of hardware and software blocks as shown in the diagrams of Figures 1, 2, and 3. The low power radio frequency (RF) signal is amplified and filtered by the receiver circuits before being digitally processed by the signal processing software. The receiver uses a high gain low noise amplifier (LNA) to provide excellent sensitivity with a characteristic noise figure of about 3 dB. The signal passes through several stages where it is down-converted, amplified and filtered by the electronics before being digitized (Figure 1). At several points in the receiver electronics, a calibrated test signal can be injected to measure the response characteristics of the receiver. After the baseband signal is digitized by an analog-to-digital

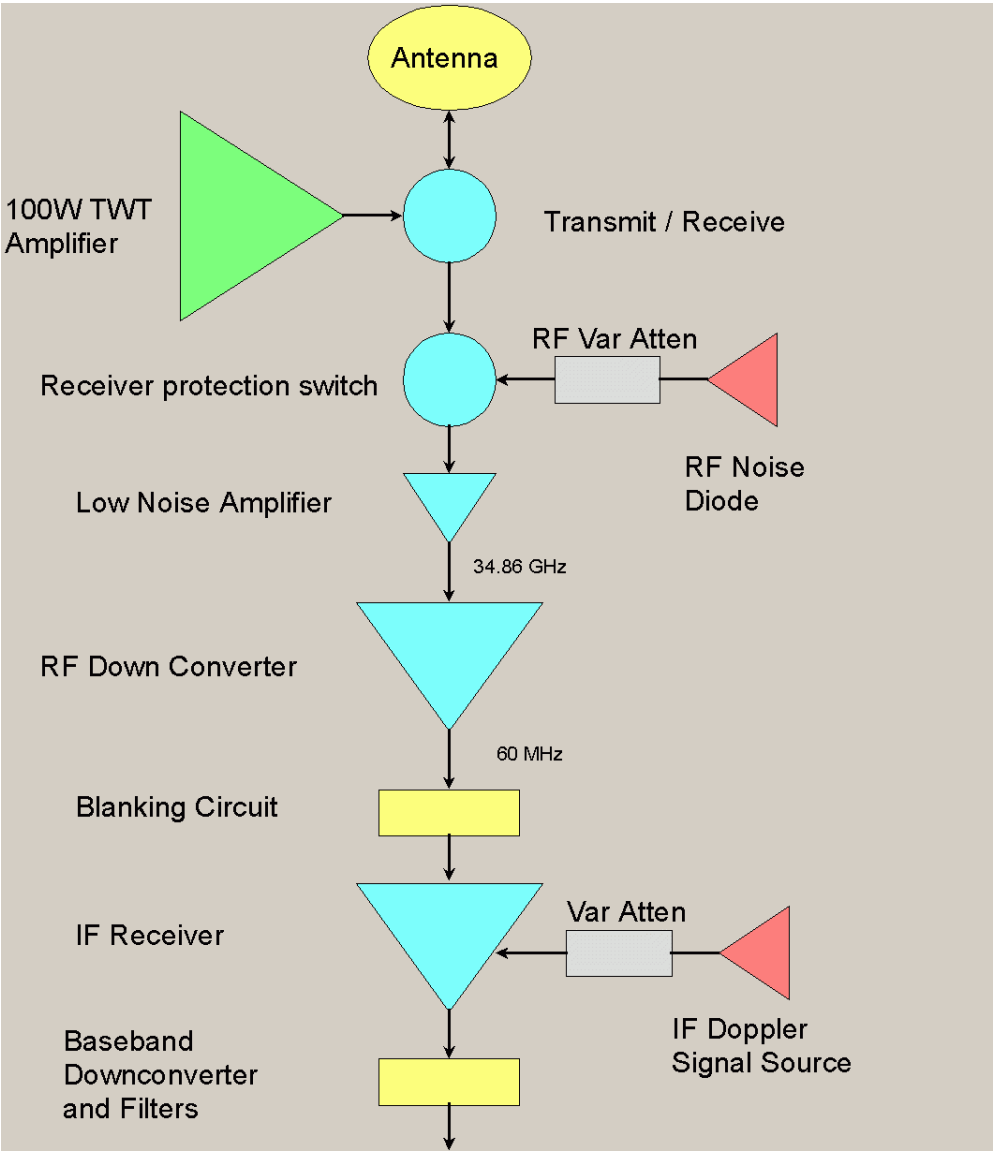

Figure 1. System level block diagram of the MMCR receiver electronics showing the RF down conversion and injected test signals used for calibration.

converter, the time series samples are summed over several radar pulses in a coherent integrator before being sent to a digital signal processing card for range processing (Figure 2). The pulse compressed time samples must be decoded in order to produce a new time series of independent range samples. Spectral processing the time series for each range gate allows for the estimation of first three moments of the Doppler spectrum. During spectral processing the DC or zero velocity component of each spectrum is independently estimated and a correction is applied to the measured value. The uncalibrated moment data is stored in files and transferred to another PC for calibration (Figure 3). The final processing of the data applies the receiver response curve for each operating mode along with a range correction formula to arrive at calibrated reflectivity estimates.

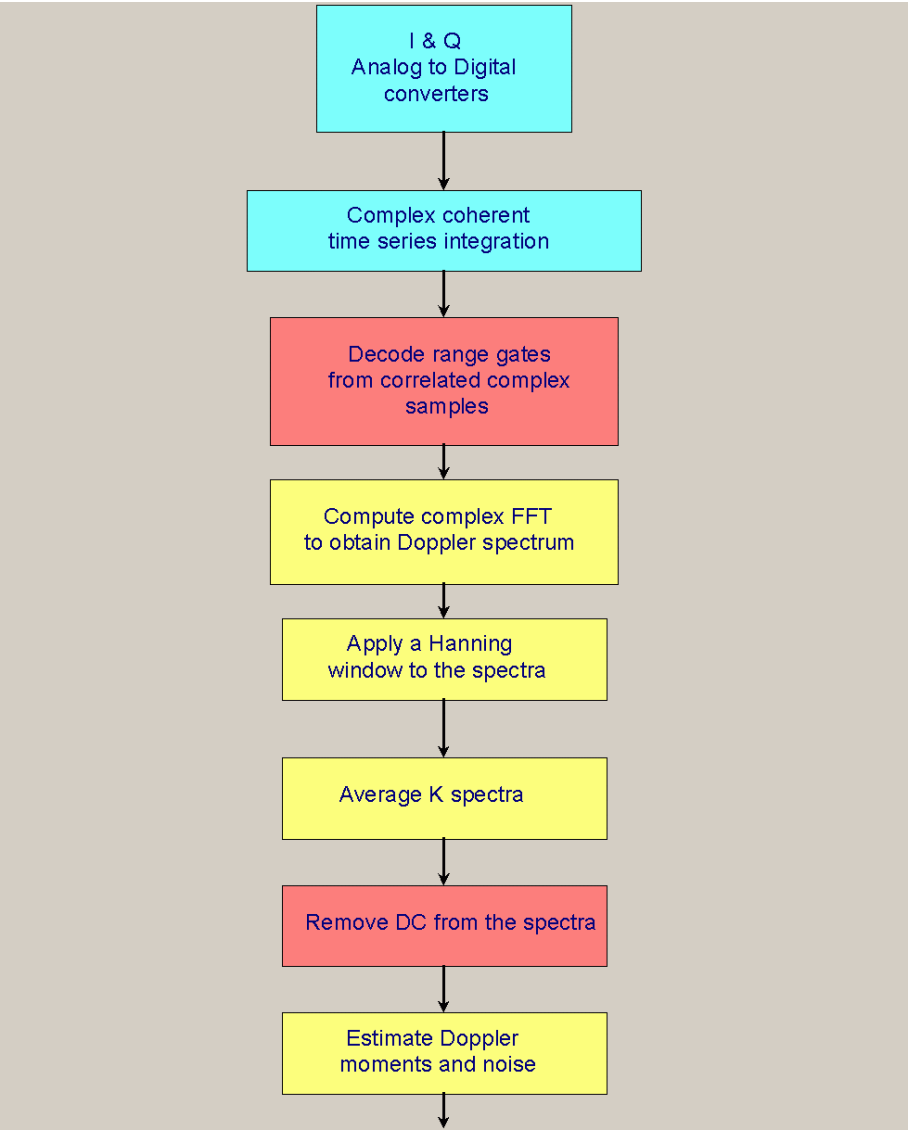

Figure 2. Digital signal processing block diagram for the MMCR. The first two steps take place in the electronic hardware and the remaining steps are performed by signal processing software.

Time Domain Coherent Integration

The time domain coherent integration technique is used to independently average the complex data samples from several radar pulses. This improves the signal-to-noise ratio of the processed signal and also reduces the number of samples in the computation of the spectral estimate, thus improving the

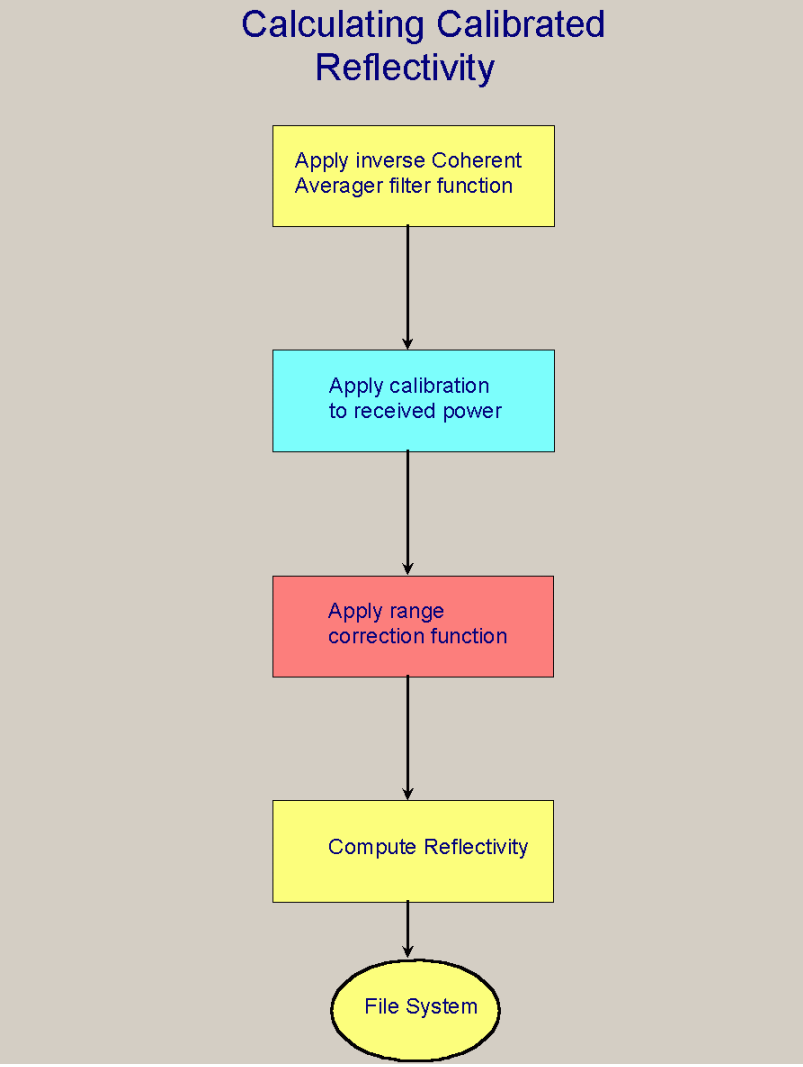

Figure 3. Steps taken to calculate calibrated reflectivity.

processing efficiency. Each point in the averaged time series represents the sum of M radar pulses. The effect of this "box car" averaging is to pass the data through a filter with a transfer function, H(ω):

$$H(\omega) = \exp\left(j(M-1)\omega\frac{\tau_o}{2} \right)\frac{\sin(M\omega(\tau_o/2))}{M\sin(\omega(\tau_o/2))}$$

where M = the number of coherent integrations
ω = the angular Doppler frequency
τ_o = the radar inter-pulse period.

Figure 4 shows the shape of the function over a normalized Nyquist velocity interval. Note that the signal rolls off to a value of 3.9 dB at the Nyquist velocity of the spectrum. The magnitude of the loss is significant for velocities greater than about 0.3 of the Nyquist interval. To compensate for this effect the inverse function is applied to the measured power estimates in the first step of the calibration process, Figure 3. The mean velocity used in the correction is taken from the first moment. In several of the operating modes the Nyquist interval is on the order of 3 ms^{-1} and echoes from lightly precipitating clouds can exceed this range. Mean velocity estimates, which are larger than the Nyquist velocity fold over in sign and the velocities and the corrected power estimates from these signals are not calibrated in the present algorithms. This effect has been reduced in the overall data by providing a separate operating mode that has a high Nyquist velocity and hence a low chance for folding.

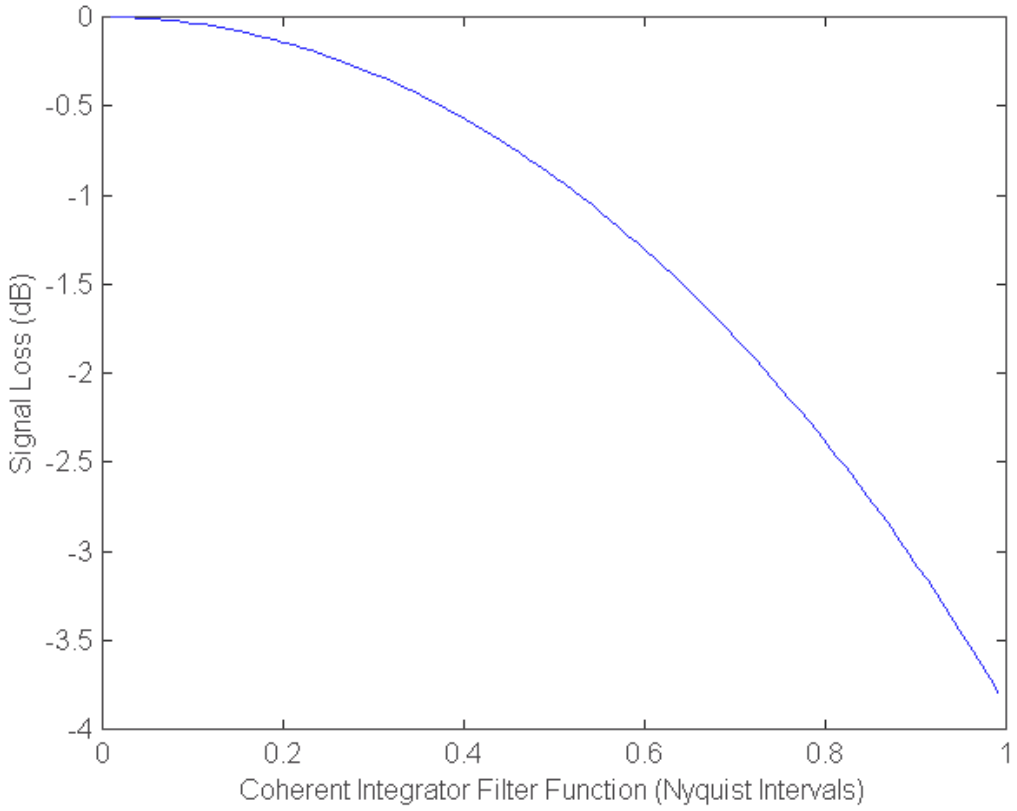

Figure 4. The magnitude of the transfer function for the time domain integrator over one Nyquist interval.

Range Decoding Artifacts Using Pulse Compression

The use of pulse compressed waveforms (complimentary pulse codes) provides increased sensitivity by using a long transmitted pulse (more average power) while maintaining the range resolution of a short pulse. The technique provides an improvement in sensitivity of 15 dB when a long pulse made up of 32 coded bits is used. The higher sensitivity allows for the detection of weak cirrus and low-level stratus clouds that would other wise go undetected by a non-pulse coded radar. Each raw time sample contains range information from N ranges (where N is the code length) convolved with the code and a

digital decoding process must be performed on the time series to arrive at the independent range samples. The decoded ranges often contain unwanted signals or artifacts from adjacent ranges when strong signal gradients or large Doppler velocities are present in the signals. Figure 5 shows the level of the leakage signal (in dB) into adjacent ranges for an 8-bit complimentary code, assuming a backscattered signal from a typical cirrus cloud. The strongest leakage is about 35 dB below the main signal. Cloud data derived from the pulse compressed signals are first passed through a threshold algorithm (Clothiaux et al. 1999) to remove any unwanted artifacts. This coded data is then combined with uncoded data from the other operating modes to provide the most sensitive observations with the fewest artifacts.

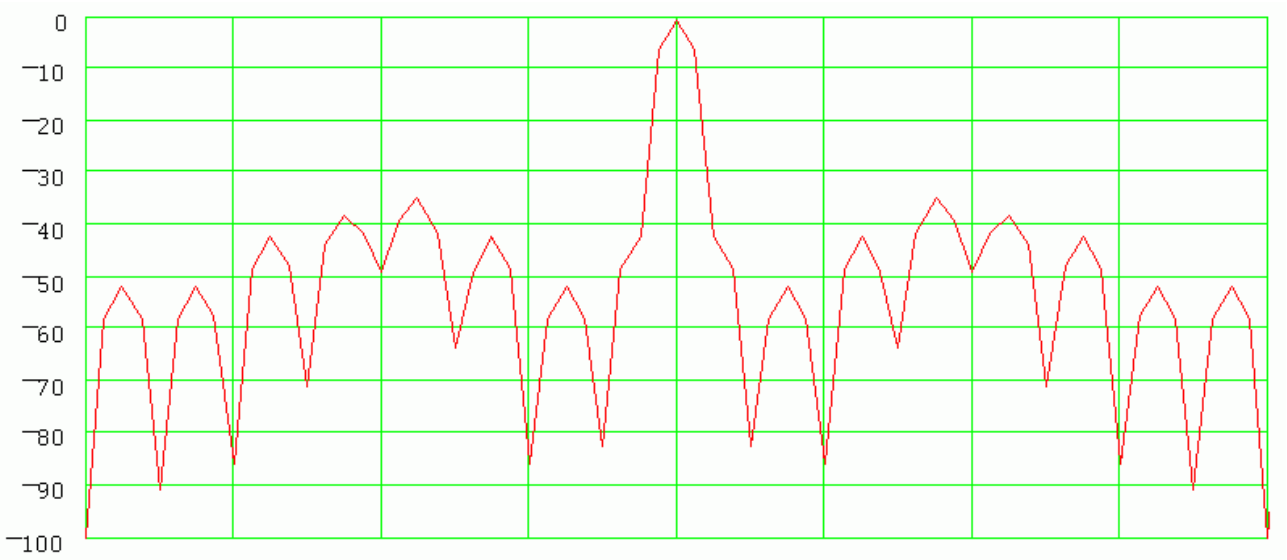

Figure 5. A plot of the computed range sidelobes for an 8-bit pulse code assuming signal conditions typical for a cirrus cloud.

DC Removal

The zero velocity point or DC component in each Doppler spectrum is often influenced by system effects. This point often is made up of two components: the signal from target echo at zero velocity and an unwanted artifact from the system DC offset, which we will term the “true DC.” The “true DC” is associated with small biases in the analog-to-digital converters or the receiver electronics and after digital processing is often much larger than the observed atmospheric signal. It is normally a requirement that this signal be removed from the spectrum before the moment estimates are made. The true DC signal power is computed as the average value of all complex time series samples (Barth et al. 1994). The DC removal algorithm computes the average value of the times series samples and subtracts it from each spectrum.

$$\text{"trueDC"} = \frac{1}{KL} \sum\sum \left(R_{jm} + iQ_{jm} \right)$$

where each real and quadrature sample, R_m or Q_m, is summed over K points per spectrum and each spectrum j, is summed over L spectrums. A Hanning window function is applied in step 5 (Figure 2) to reduce sidelobes in the spectrum caused by the finite length of samples. This window has the affect of spreading a small amount of the DC signal into the two adjacent spectral bins. The DC removal software applies a correction to the two spectral points.

Radar Calibration

One of the underlying goals in the use of MMCR data is to make accurate reflectivity measurements to better understand the distribution and concentration of different types of cloud particles. Accurate reflectivity measurements require that a good calibration of the radar system be made at regular intervals. Typically, radars with scanning antennas use a direct method of calibration that relies on measuring the return signal from a calibrated corner reflector of known cross section (Sekelsky and MacIntosh 1996). The antenna is pointed at the elevated corner reflector and the reflectivity measurements can be inferred directly from the backscattered signal. The MMCR, however, has a fixed position vertically pointing antenna, which rules out the use of the direct method, and in its place we use an indirect method. This relies on making a separate calibration of each of the major components in the radar, which include:

- transmitter RF power
- antenna gain
- system losses
- receiver/processor gain.

Because there are more measurements required in this technique, the uncertainties of the indirect method are usually larger than the direct method, and therefore, presumably, less accurate. The measurements of the RF power, system losses and receiver/processor gain can be made using standard techniques but the direct measurement of the antenna gain is normally made on a specialized test range. Therefore the antenna gain measurement is usually made only once during manufacture and is rarely made once the system has been deployed. Usually the biggest unknown in any of the measurements is the antenna gain and the substitution of a small calibrated antenna for the standard antenna can also be made to validate the system's calibration. In the field, the radar calibrations need periodic validation and one technique that is often used is the comparison with other radars. Comparisons between radars that agree within 1 db to 2 dB are considered quite good.

Measurement of the system losses and transmitted power in the MMCR are done routinely but the measurement of the receiver and signal processor requires several automated steps to characterize the response curve, Figure 6. The curve is a measure of the total signal gain through the combined signal path of the receiver and the signal processor and relates the computed output power to the calibrated input signal. The linear region in the center of the curve is obtained from measurements using a calibrated noise source injected ahead of the RF pre-amp (Figure 1). A variable RF attenuator is used to

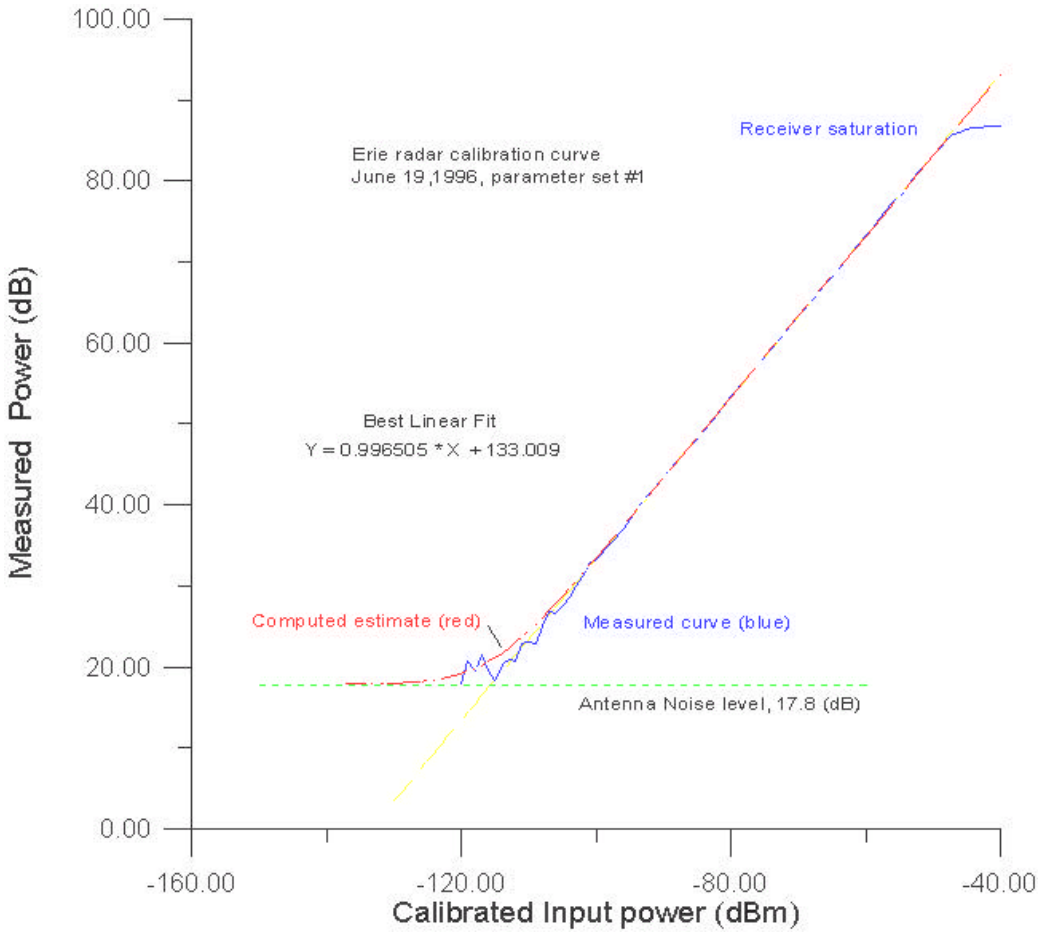

Figure 6. The receiver and signal processor characteristic response curve derived from a calibrated noise source.

step the noise signal level through about a 20-dB region above the knee in the curve to obtain a best linear fit. The calibrated output power of the noise diode as measured by the receiver and processor is given by:

$$\text{Noise Power} = 10\log\left(\frac{kT\Delta B}{NTDCI}\right) + \text{ENR} - \text{RFAtten}$$

where
- k = Boltzman's constant
- T = the ambient temperature
- ΔB = the receiver bandwidth
- NTDCI = the number of time domain coherent integrations
- ENR = the excess noise ratio (available noise power) of the calibrated noise diode
- RFAtten = the attenuator setting.

The calibration relies on accurate estimates by the processor of the system noise power.

The knee in the lower part of the curve is estimated from the minimum receiver noise measured at the antenna terminal. Receiver saturation occurs in the upper part of the curve and is measured using a high level IF signal injected into the IF section of the receiver. The MMCR receiver has a typical dynamic range of about 65 dB between the minimum detectable signal and the start of receiver saturation. The total response curve is stored in the calibration software table. Calibrated power measurements are obtained by applying the response curve to the values measured by the radar processor.

Range Correction Formula

Most radar antennas are designed to work in the far field, where plane wave propagation is assumed. For the MMCR with a 3-m diameter antenna, a midpoint between the near-to-far field transition is roughly located at 1 km and the radar routinely sees clouds below this region. A modified version of the radar range formula has been developed to help interpret reflectivity measurements within the near field region (Lataitis et al. 1998). The formula is expressed in a standard form that is valid from the near field into the far field so that it can be applied at any range.

$$\text{Range Correction Formula} = R^2 \bullet \left(1 + \left[0.63 \frac{D_o}{\sqrt{\lambda \bullet R}} \right]^4 \right) \text{where } D_o = \frac{\lambda}{\pi} \sqrt{G_o}$$

where D_o = the effective diameter of the antenna
λ = the radar wavelength
R = the range to the sampling volume
G_o = the measured antenna gain.

Reflectivity Equation

The formula for the effective reflectivity factor (in dB) is commonly expressed in terms of the received power, the range correction and a radar constant:

$$dBZ_e = 10\log Z_e = 10\log (P_r) + 10\log (\text{RangeCorrectionFormula}) + 10\log (\text{RadarConstant})$$

$$\text{Radar Constant} = \frac{512 \ln 2 \, \lambda_r^2 \, L_{sys}}{P_t \, G_o^2 \, \theta\phi \, \Delta R \, \pi^3 \, |K|^2 \, \text{CODE}} 10^{18}$$

where Z_e = effective reflectivity factor ($mm^6 m^{-3}$)
P_r = received peak power (mw)
R = range to the sampling volume (m)
λ_r = radar wavelength (m)
L_{sys} = system losses
P_t = transmitted peak power (mw)
G_o = antenna gain
θ, ϕ = antenna beamwidths (radians)

ΔR = range resolution (m)
$|K|^2$ = 0.93, index of refraction of water
CODE = number of code bits used.

The formula can be applied to all the radar operating modes including the modes using pulse compression. The received peak power is obtained by applying the receiver calibration curve to the measured power, Figure 3, step 2. The system losses include the measured waveguide losses as well as the computed matched filter loss in the receiver.

Summary

The MMCR signal processing encompasses the use of coherent pulse integration, pulse compression and a range formula for the antenna to account for the effects of the near field regions. We have reviewed many of the basic processing blocks used in the radar with the aim of giving an understanding of the corrections applied to the data to arrive at accurate reflectivity estimates of the clouds.

References

Barth, M. F., R. B. Chadwick, and D. W. van de Kamp, 1994: Data processing algorithms used by NOAA's wind profiler demonstration network. *Ann. Geophysicae*, **12**, 518-528.

Clothiaux, E. E., K. P. Moran, B. E. Martner, T. P. Ackerman, G. G. Mace, T. Uttal, J. H. Mather, K. B. Widener, M. A. Miller, and D. J. Rodriguez, 1999: The atmospheric radiation measurement program cloud radars: operational modes. *J. Atmos. Oceanic Technol.*, **16**, 819-827.

Lataitis, R. J., R. G. Strauch, K. P. Moran, and B. E. Martner, 1998: Near-field correction to the meteorological radar equation. *Proc. 4th Intl. Symp. On Troposheric Profiling*, Snowmass, Colorado, 188-190.

Moran, K. P., B. E. Martner, M. J. Post, R. A. Kropfli, D. C. Welsh, and K. B. Widener, 1998: An unattended cloud-profiling radar for use in climate research. *Bull. Amer. Meteor. Soc.*, **79**, 443-455.

Sekelsky, S., and R. MacIntosh, 1996: Cloud observation with a polarimetric 33-GHz and 95-GHz radar. *Meteor. Atmos. Phys.*, **59,** 123-140.